◆ Human Brain Mapping 35:1284–1296 (2014) ◆

# Dysmaturation of the Default Mode Network in Autism

**Stuart D. Washington,[1,2,3]* Evan M. Gordon,[4] Jasmit Brar,[1,2] Samantha Warburton,[1,2] Alice T. Sawyer,[1,2] Amanda Wolfe,[1,2] Erin R. Mease-Ference,[1,2] Laura Girton,[1,2] Ayichew Hailu,[1,2] Juma Mbwana,[1,2] William D. Gaillard,[3] M. Layne Kalbfleisch,[1,5] and John W. VanMeter[1,2]***

[1]*Center for Functional and Molecular Imaging, Georgetown University Medical Center, Washington, District of Columbia*
[2]*Department of Neurology, Georgetown University Medical Center, Washington, District of Columbia*
[3]*Children's National Medical Center, Northwest, Washington, District of Columbia*
[4]*Interdisciplinary Program in Neuroscience, Georgetown University Medical Center, Washington, District of Columbia*
[5]*Krasnow Investigation of Developmental Learning and Behavior, Fairfax, Virginia*

**Abstract:** Two hypotheses of autism spectrum disorder (ASD) propose that this condition is characterized by deficits in Theory of Mind and by hypoconnectivity between remote cortical regions with hyperconnectivity locally. The default mode network (DMN) is a set of remote, functionally connected cortical nodes less active during executive tasks than at rest and is implicated in Theory of Mind, episodic memory, and other self-reflective processes. We show that children with ASD have reduced connectivity between DMN nodes and increased local connectivity within DMN nodes and the visual and motor resting-state networks. We show that, like the trajectory of synaptogenesis, internodal DMN functional connectivity increased as a quadratic function of age in typically developing children, peaking between, 11 and 13 years. In children with ASD, these long-distance connections fail to develop during adolescence. These findings support the "developmental disconnection model" of ASD, provide a possible mechanistic explanation for the Theory-of-Mind hypothesis of ASD, and show that the window for effectively treating ASD could be wider than previously thought. *Hum Brain Mapp 35:1284–1296, 2014.* 

**Key words:** autism; default mode network; functional connectivity; development; Theory of Mind; synaptogenesis

Additional Supporting Information may be found in the online version of this article.

Contract grant sponsor: NICHD; Contract grant number: T32HD046388 (Dr. Washington by way of a post-doctoral training award, V.G.); Contract grant sponsor: STAART (Johns Hopkins University's Kennedy-Krieger Institute); Contract grant number: NIH/NIMH IU54MH066417-01, R.L.); Contract grant sponsor: Intellectual and Developmental Disorders Research Center; Contract grant number: NIH/NICHD 2P30HD040677-06; Contract grant sponsor: Georgetown General Clinical Research Center; Contract grant number: NIH/NCRR 5M01RR023942-03

*Correspondence to: Stuart D. Washington and John W. VanMeter, Room LM14, Preclinical Sciences Building, Georgetown University Medical Center, 3900 Reservoir Rd NW, Washington, DC 20057, USA; E-mail: sdw4@georgetown.edu; jwv5@georgetown.edu

Received for publication 24 October 2012; Accepted 10 December 2012

DOI: 10.1002/hbm.22252

Published online 18 January 2013 in Wiley Online Library (wileyonlinelibrary.com).

## INTRODUCTION

The self-reflective thought processes necessary for viewing situations from the perspectives of others (Theory of Mind) typically begin developing during childhood and continue through adulthood [Dahlgren et al., 2010; Lackner et al., 2010; Lombardo et al., 2010]. In typically developing (TD) children, the majority of cortical networks follow a quadratic trajectory of synaptogenesis that peaks between the ages 11 and 13 years [Giedd et al., 1999; Gogtay et al., 2004; Lenroot and Giedd, 2006]. Individuals diagnosed with autism spectrum disorder (ASD) often exhibit impairments in Theory of Mind [Baron-Cohen, 1989; Boucher, 1989; Colle et al., 2007] and other such tasks involving mental simulation of alternative perspectives [Ben Shalom, 2003].

The "developmental disconnection model" links symptoms of ASD to weak functional connectivity between remote, and an overabundance of functional connectivity within local, cortical regions [Belmonte et al., 2004; Belmonte and Yurgelun-Todd, 2003; Damarla et al., 2010; Geschwind and Levitt, 2007; Just et al., 2004]. The default mode network (DMN) is most active at rest, is involved in such self-reflective and social cognition as episodic memory [Addis et al., 2007; Greicius and Menon, 2004; Kim, 2010; Kim et al., 2010], prospection [Addis et al., 2007], and Theory of Mind [Saxe and Kanwisher, 2003; Spreng and Grady, 2010], and is comprised of several dispersed cortical nodes including the anterior cingulate/medial prefrontal cortices and the posterior cingulate cortex (PCC) among others [Buckner et al., 2008; Greicius et al., 2003; Greicius and Menon, 2004; Raichle et al., 2001]. Evidence suggests that weak functional connectivity between DMN nodes underlies deficits in self-reflective and social cognition observed in ASD [Assaf et al., 2010; Stigler et al., 2011]. Contactin-associated protein-like 2 (CNTNAP2) has been linked this protein to deficits in neuronal synchrony in a knock-out mouse model of autism [Penagarikano et al., 2011] and in humans [Scott-Van Zeeland et al., 2010].

We conducted resting-state functional magnetic resonance imaging (fMRI) analyses of data from both TD children and those with ASD to ascertain differences in DMN functional connectivity between the two groups. We demonstrate that not only are functional connections between DMN nodes in children with ASD weak relative to those of age-matched TD children but also that these connections do not mature quadratically as they do in TD children. Correlations with autism psychometrics showed a relationship between decreased functional connectivity and increased ASD symptom severity, especially in the social and communication domains.

## METHODS

### Subjects

Twenty-four children (21 males, 3 females) previously diagnosed with ASD participated in this study, and 24 TD children (21 males, 3 females) who were age-matched to the ASD group served as control subjects. Hereafter, we refer to the complete set of age-matched controls as the $TD_{match}$ group. The $TD_{match}$ group was further divided into two subgroups based on subject age: the $TD_{6–9}$ group (composed of 12 children aged 6–9 years) and the $TD_{10–17}$ (composed of 12 children age 10–17 years). In accordance with Georgetown University Medical Center IRB-approved protocols, written parental consent was obtained following explanation of experimental procedures to parents and children provided their assent, and the families of each participant were compensated.

ASD group had their symptoms treated using a variety of psychoactive medications. Nine subjects in our ASD group were not on any psychoactive drugs. Five subjects in our ASD group were taking selective serotonin reuptake inhibitors (SSRIs), another nine were taking psychostimulants, two were taking antipsychotics, and one was taking an atypical antidepressant (Bupropion). Seven of these subjects were using more than one of the drugs listed above.

### Demographics and Behavioral Testing

We obtained the following information for each subject: age, sex, handedness, and IQ score (Wechsler Abbreviated Scale of Intelligence, WASI). The ASD and $TD_{match}$ groups did not significantly differ in age. The ASD group did not significantly differ in performance IQ from either the $TD_{match}$ or $TD_{6–9}$ groups, but, as expected, displayed significantly ($P < 0.05$) lower verbal and total IQ scores.

All ASD subjects met diagnostic criteria for ASDs based on several measures. The Social Communication Questionnaire (SCQ) was administered to the parents of all participants in part to verify that both groups of TD subjects were not on the autism spectrum. SCQ scores for the $TD_{match}$ ($2.04 \pm 1.82$ SD) and $TD_{6–9}$ ($2.3 \pm 1.64$ SD) were significantly ($P < 0.01$) lower than those of the ASD group ($17.88 \pm 4.80$ SD). Clinicians assessed 17 of the ASD subjects using the Autism Diagnostic Interview-Revised (ADI-R) [Lord et al., 1994] and the Autism Diagnostic Observation Schedule (ADOS) [Lord et al., 2000]. Each of these subjects met the ADI-R and ADOS criteria for ASD. In addition, 10 ASD subjects were tested using the Social Responsiveness Scale, or SRS [Constantino and Gruber, 2005]. SCQ scores were greater ($P < 0.01$) among children with ASD than among TD children. Demographic and behavioral information for all subject groups are summarized in Tables I and II.

### Task

We obtained resting-state data from our subjects by analyzing BOLD fluctuations associated with the fixation condition blocks of a modifier flanker task [a version of the Naglieri Nonverbal Ability Test (NNAT) licensed to Dr. Kalbfleisch] following previously used methods [Fair

**TABLE I. Subject demographics**

| Subjects ($N = 48$) | $TD_{match}$ ($N = 24$) | ASD ($N = 24$) |
|---|---|---|
| Age | 10.08 ± 3.17 SD | 10.88 ± 2.27 SD |
| Sex | 21 M, 3 F | 21 M, 3 F |
| Handedness | 23 R, 1 L | 23 R, 1 L |
| Full-scale IQ | 123.44 ± 10.54* SD | 113.17 ± 18.93 SD |
| Performance IQ | 118.67 ± 12.43 SD | 112.04 ± 16.47 SD |
| Verbal IQ | 120.76 ± 9.13* SD | 110.42 ± 20.37 SD |
| Full-scale SCQ | 1.67 ± 1.39 SD | 17.88 ± 4.80** SD |

* ($P < 0.05$); ** ($P < 0.01$).

et al., 2008]. The stimuli in the modified flanker task consisted of presentations of a 3 × 3 arrays of block arrows (Fig. 1). Subjects were instructed to respond based on the orientation of the center arrow using a set of button boxes. The experiment was presented in 48-s blocks. There were four fixation blocks for a total nontask time of 3 min, 12 s.

## Data Acquisition

Imaging was performed using a 3-T whole-body MRI scanner (Siemens Magnetom Trio, Erlangen, Germany) and a circularly polarized head coil. Head movement was minimized by padding that firmly yet comfortably held the subject's head still in the coil.

### *Functional MRI data*

Subjects were scanned during performance of the modified flanker task using an echo-planar imaging (EPI) sequence sensitive to blood-oxygenation level-dependent (BOLD) contrast with the following parameters: TR = 3,000 ms, TE = 30 ms, flip angle = 90°, matrix size = 64 × 64, FOV = 192 × 192 $mm^2$, 50 slices with a thickness of 2.8 and a 0.2-mm gap for an effective resolution of 3.0 × 3.0 × 3.0 $mm^3$ for a total run time of 6 min, 33 s.

### *Structural MRI data*

Neuroanatomical localization of BOLD activity was determined using a structural protocol consisting of a magnetization prepared-rapid acquisition gradient echo (MP-RAGE) scan acquired during the same scanning session with the following parameters: TR = 1,600 ms, TE = 4.38 ms, TI = 640 ms, flip angle 15°, averages = 1, 160 slices with a 1.0-mm thickness, FOV = 256 × 256 $mm^2$, effective resolution = 1.0 × 1.0 × 1.0 $mm^3$, scan time = 6:51 min. All structural scans were examined for gross neurological findings.

## Data Analysis

### *Preprocessing*

fMRI scan data were preprocessed using SPM5 (Wellcome Department of Cognitive Neurology, London, UK). The first three volumes (9 s) of each functional run were discarded to allow for equilibrium in longitudinal magnetization. The images were corrected for differences in slice acquisition times and then were spatially realigned to the first volume to correct for head motion. The functional images were spatially normalized using the EPI template from SPM5, and smoothed with a Gaussian kernel of 9 mm. Based on analysis of motion using ArtRepair (threshold of 10% of scans per subjects having >1.5% average global whole volume signal change), subjects who exhibited large motion artifacts were excluded from all groups. Two volumes at the beginning of each fixation block were removed, leaving 14 volumes (42 s) per fixation block to avoid contamination by lagging, task-related hemodynamic changes [Fair et al., 2007]. These shortened fixation blocks were concatenated for further analysis.

### *Independent components analysis*

Independent components analysis (ICA) is a statistical process of tensor multiplication that separates a set of signals into independent, uncorrelated, and non-Gaussian spatiotemporal components [Comon, 1994]. ICA is now commonly used to identify low-frequency fluctuations in BOLD-signal associated with resting-state networks [Raichle et al., 2001; Tyler et al., 2008]. We used "Multi-Session Temporal Concatenation" within FSL MELODIC (www.fmrib.ox.ac.uk/fsl/melodic2/index.html) to perform separate group-ICAs on the concatenated fixation blocks from all TD groups and our ASD group. We chose not to impose a predetermined number of independent components and permitted MELODIC to automatically estimate the dimensionality of the data and the number of components generated for all TD groups and for the ASD group. We then visually identified which of these maps corresponded to the DMN by visually comparing each map to published atlases [Raichle et al., 2001].

### *Region-of-interest analysis*

To directly measure differences in functional connectivity between specific nodes within DMN between our ASD group and all TD groups, we conducted temporal

**TABLE II. Autism Psychometric scores**

| | |
|---|---|
| ADI-R (N=17) | ADI-Abn (2.8 ± 1.5 s.d.) |
| | ADI-Comm(17.2 ± 5.0 s.d.) |
| | ADI-Rep Beh (7.9 ± 2.6 s.d.) |
| | ADI-Soc (19.8 ± 5.7 s.d.) |
| ADOS (N=17) | ADOS-comm (4.2 ± 1.2 s.d.) |
| | ADOS-Imag (1.0 ± 0.6 s.d.) |
| | ADOS-Soc (8.7 ± 2.5 s.d.) |
| | ADOS-Stereo Beh (2.8 ± 1.6 s.d.) |
| SRS (N±10) | SRS-Cogn (4.2 ± 1.2 s.d.) |
| | SRS-Comm (8.7 ± 2.5 s.d.) |
| | SRS-Mann (2.8 ± 2.8 ± 1.6 s.d.) |
| | SRS-Motv (1.0 ± 0.6 s.d.) |

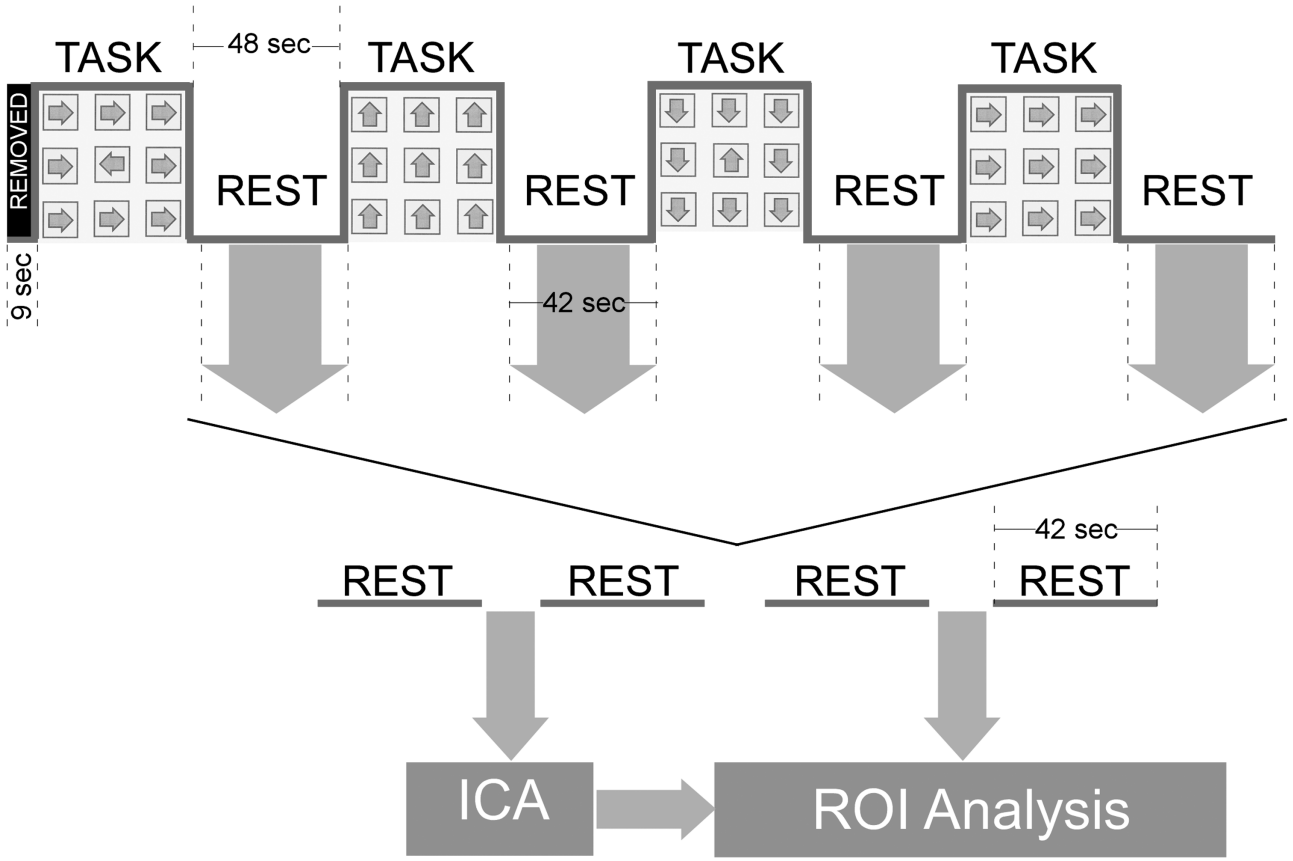


**Figure 1.**

Illustration of the experimental design and subsequent data analysis. fMRI data in this study was elicited by BOLD signal fluctuations associated with the fixation blocks of a modified, flanker task presented using a block design. For the purposes of this study, changes in BOLD signal were only measured from scans associated with the 48-s control period (i.e., rest block), and scans associated with the performance/perception of the modified flanker task and its stimuli were discarded. BOLD activity associated with resting-state networks was visually identified using an ICA analysis. ROIs were created based on loci of BOLD activity in the $TD_{match}$ group that were associated with nodes of the default mode network (DMN), and correlations (Fisher's *Z*-scores) of BOLD signal fluctuations between DMN nodes were used to determine functional connectivity.

correlations of the signal time courses within specific regions of interest (ROIs). We used MRIcron (www.nitrc.org/projects/mricron) to identify, based on a threshold of 87.5%, or seven-eighths, of ICA map maximum, ROIs corresponding to the DMN nodes. The ROIs were constructed from these demarcated regions using the MarsBaR (MARSeille Boîte À Région d'Intérêt; www.mrc-cbu.cam.ac.uk/Imaging/marsbar.html) toolkit within SPM [Brett et al., 2002].

We based our ROIs on maps generated by ICA to avoid biasing our analyses with "a priori" hypotheses. We based all of our comparisons of traditional DMN nodes (ACC/mPFC, PCC, and bilateral MTG and IPL) on ROIs constructed from the single map output from group-ICA of the $TD_{match}$ group. A split within the ACC/mPFC node in the ASD subjects necessitated the construction of ROIs based on ICA results from the ASD group. To this end, we created ROIs based on the ventral and dorsal portions of the ACC/mPFC node in the ASD group. We called these the vACC/mPFC and dACC/mPFC nodes, respectively.

For each default mode ROI, the residual time courses for each voxel within an ROI were averaged, and the mean residual time courses within each pair of ROIs were then correlated against each other in a pairwise fashion to assess functional connectivity. This procedure generated a correlation value (Pearson's *r* converted to Fisher's *Z*) reflecting the strength of functional connectivity between each ROI pair. Finally, we correlated behavioral measures of ASD deficits (e.g., ADOS, ADI-R, SRS, and SCQ) and demographic measures (e.g., age) with measures of functional connectivity. To minimize the effect of physiological

factors (such as respiration or heart rate) common to the time courses of all ROIs, we regressed out the signal time course from non-neuronal sources, specifically from cerebral spinal fluid and white matter [Van Dijk et al., 2010].

### *Dual-regression analysis*

A dual regression analysis was performed to determine differences in degree of connectivity within nodes between groups of subjects. The dual-regression analysis proceeded in three steps: (1) spatial regression: for each subject, the full set of component maps from that group's ICA was used as regressors in a spatial multiple regression conducted on each time point of the subject's preprocessed resting data. This regression returned a set of beta values, each of which represent the degree to which one component can explain the spatial pattern of activity at one time point. Conducted over all time points in the subject's data, this analysis returns time courses representing the temporal dynamics of each group's identified component. (2) Temporal regression: the full set of component time courses was used as regressors in a temporal multiple regression conducted voxelwise on the subject's preprocessed rest data, using SPM5. This analysis results in a set of spatial maps for each subject, each of which represents that subject's version of one known group-level ICA component. (3) Identification of group effects: for all of the components of interest, the corresponding subject-level spatial component maps were entered into a voxelwise two-sample *t*-test within SPM5 to test for differences in the ICA-derived connectivity of that component between the TD and ASD groups. Resultant images were thresholded using a family-wise error (FWE) correction of $P < 0.05$.

## RESULTS

### Internodal DMN Connectivity in Typically Developing Children versus Those With Autism Spectrum Disorder

We first analyzed fMRI data from 24 children with ASD and 24 ($TD_{match}$) children. To avoid imposing "a priori" hypotheses on the analysis of fMRI data, we used ICA to generate separate component maps for different neuronal networks as well as for motion artifact and physiological noise [Beckmann et al., 2005; Beckmann and Smith, 2005]. Using previously described methodology, we identified which of the maps delineated DMN and other resting-state networks [Gordon et al., 2011; Kiviniemi et al., 2009].

Group-ICA generated a total of 20 components (functional connectivity maps) for the ASD group and 13 for the $TD_{match}$ group. Among these components were functional connectivity maps consistent with visual, motor, and default-mode networks (DMN) in both the ASD and $TD_{match}$ groups. DMN, comprising nodes within the anterior-cingulate/medial prefrontal cortex (ACC/mPFC), precuneus cingulate cortex/PCC, bilateral middle temporal gyrus (MTG), and bilateral inferior parietal lobule (IPL) appeared as a single component in the $TD_{match}$ group (Fig. 2a). In the ASD group, however, DMN separated into three different components (Fig. 2b). The dorsal and ventral extents of the ACC/mPFC node split into two separate components in the ASD group. The ventral ACC/mPFC (vACC/mPFC) node of the ASD group was encompassed within the same component as the MTG nodes whereas the dorsal ACC/mPFC (dACC/mPFC) node was in a separate component. The PCC node alone comprised a third independent component in the ASD group.

Remaining components in the $TD_{match}$ group included motion artifact (4/13 components) and physiological activity (including vascular, cerebral–spinal, and eye movement activity, 6/13), as well as the visual (1/13) and motor (1/13) resting-state networks. In the ASD group, the remaining components included motion artifact (7/20), physiological activity (7/20), as well as non-DMN-associated bilateral posterior parietal (1/20), left angular gyral (1/20), motor (1/20), auditory (1/20), and visual (1/20) resting-state networks.

To investigate more fully the functional connectivity among DMN nodes in the ASD and $TD_{match}$ groups, we performed correlations of BOLD signal time courses between ROIs in a pairwise fashion. All ROIs were based upon nodes from the $TD_{match}$ group's ICA component map. DMN functional connectivity analyses are summarized in Figure 2a for the $TD_{match}$ group and Figure 2b for the ASD group. Post-hoc analyses (Fig. 2c, right) revealed a difference ($P < 0.05$) in functional connectivity between the $TD_{match}$ and ASD groups.

We tested for differences between groups on internodal functional connectivity within DMN using a $2 \times 2$ random effects analysis of variance (ANOVA) with group ($TD_{match}$ and ASD; between subjects; for both groups, $n = 24$) and network connection (within subjects) as factors. There was a main effect of group, such that $TD_{match}$ subjects had generally greater DMN connectivity than ASD subjects ($F[1, 690] = 53.60$, $P < 0.01$). There was also a main effect of ROI connectivity, such that certain pairs of regions had greater functional connectivity than others ($F[14, 690] = 4.15$, $P < 0.01$). The lack of an interaction effect between group and ROI connectivity ($F[14, 690] = 0.66$, $P = 0.81$) indicated that functional connectivity differences between the $TD_{match}$ and ASD groups were largely ubiquitous across all pairings of DMN nodes. Notably, all significant functional connectivity differences between $TD_{match}$ and ASD groups are due to stronger internodal DMN connectivity among $TD_{match}$ subjects.

We studied connectivity between the dACC/mPFC and vACC/mPFC regions for both groups as a post-hoc analysis. There was significantly greater ($P < 0.05$) functional connectivity among $TD_{match}$ than among ASD subjects between these regions as shown in Supporting Information Figure SS1.

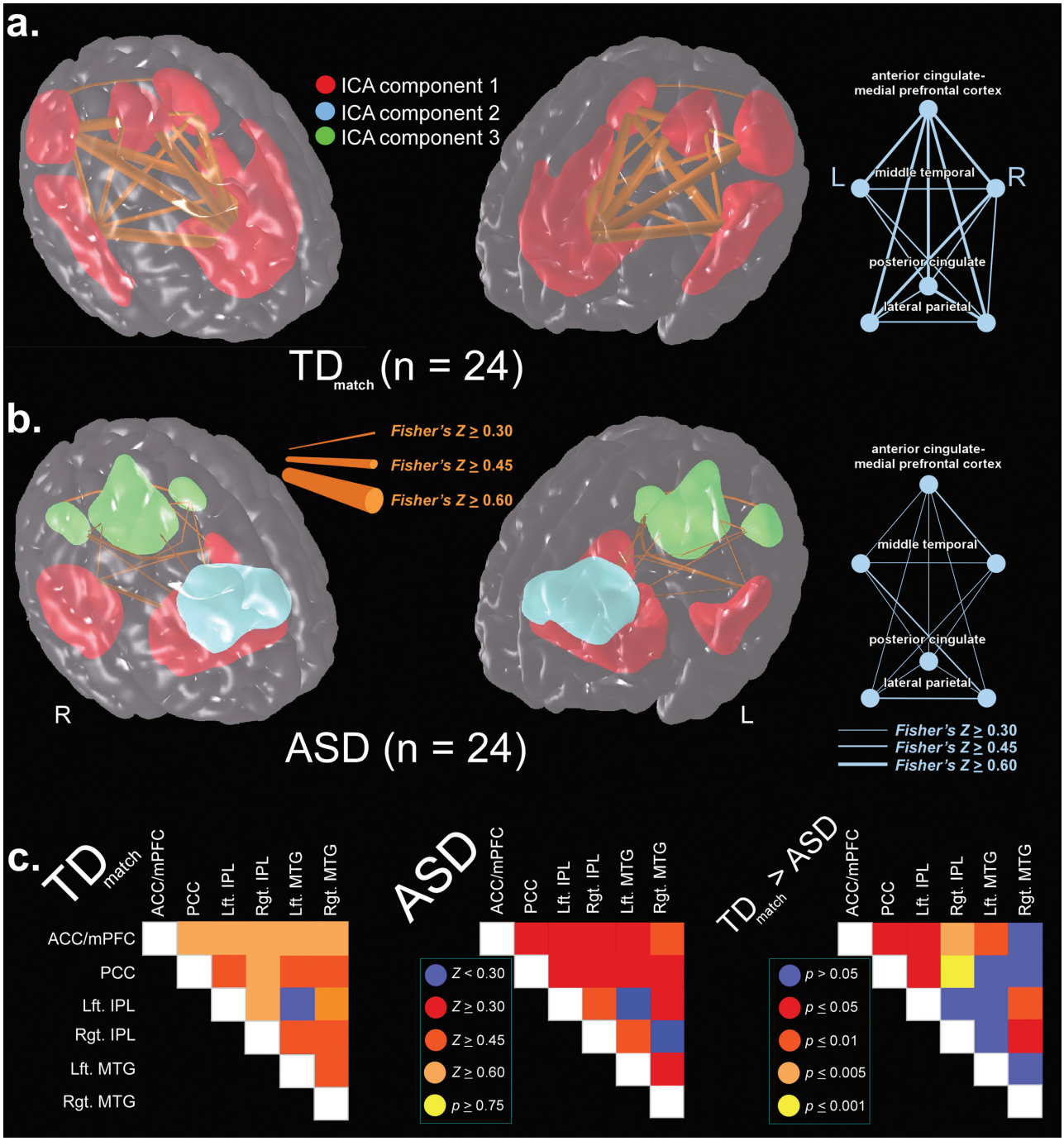


**Figure 2.**

Comparisons between the internodal DMN functional connectivity of children with ASD and age-matched TD children ($TD_{match}$). Three-dimensional renderings of the functional connectivity between DMN nodes in the $TD_{match}$ group (a) and the ASD group (b) visualized in a translucent brain template are shown in the left and middle figures. Regions-of-interest (ROI) were determined in an unbiased, data-driven approach using ICA on four rest blocks (each 42 s) of a modified flanker task. Colors of ROIs denote the different independent components identified in each group. Strengths of functional connections were ascertained using average partial correlations of BOLD signal between the ICA-derived ROIs and are depicted by the width of the lines connecting pairs of nodes. The right figure shows a top-down 2D graphical depiction of the functional connections between DMN nodes as determined by partial correlations in which line-widths denote strengths of functional connections. As the complete DMN was contained in a single ICA component in the $TD_{match}$ group, all of these ROIs are shown in red (a). In the ASD group (b), three ICA components were needed to identify the DMN: the red (ventral ACC/mPFC and MTG), cyan (dorsal ACC/mPFC), and green (PCC and IPL) ROIs. (c) Left: Correlation matrix representing DMN functional connectivity for the $TD_{match}$ group. Colors correspond to Fisher's *Z* transformations of Pearson's Product moment correlations. Middle: correlation matrix of default mode functional connectivity for children with ASD. Representation is similar to that at left. Right: Matrix representation of post-hoc statistical comparisons between DMN functional connectivity in the $TD_{match}$ and ASD groups. Representations match those above except that colors symbolize *P* values as opposed to Fisher's *Z* values. Connectivity differences between the $TD_{match}$ and ASD groups are shown in detail in Supporting Information Figure SS2.

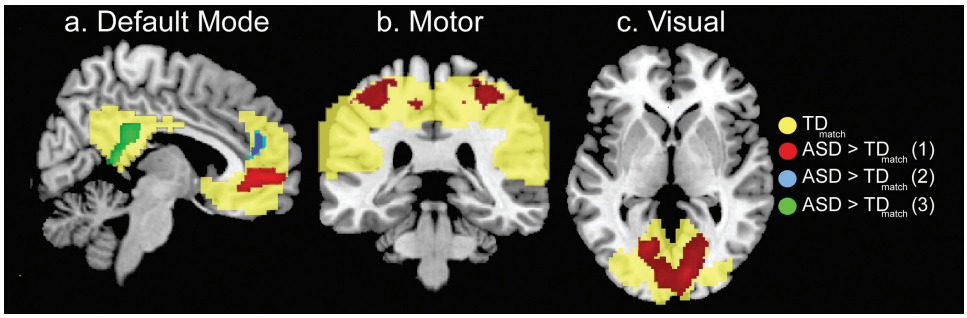


**Figure 3.**

Differences in intra-nodal (a) DMN, (b) motor, and (c) visual network functional connectivity between TD children and those with ASD. Translucent yellow regions represent ICA-derived ROIs based on results from the $TD_{match}$ group, and correspond to DMN (left), motor (middle), and visual (right) networks, each of which could be described by a single ICA component. Red, cyan, and green regions, respectively, represent voxelwise dual-regression comparisons (ASD > $TD_{match}$) between the first, second, and third components from the ASD group and the single ICA-component from the $TD_{match}$ group. In the ASD group, only the DMN required more than one ICA-component to describe the entire network. Voxelwise comparisons were predicated on performing dual regression on each subject's resting-state data and were masked by the DMN, motor, and visual networks of the $TD_{match}$ group and thresholded at $P < 0.05$ (FWE corrected; extent threshold = 50 voxels). The inverse comparison ($TD_{match}$ > ASD) yielded no significant voxels in either the motor or visual networks, and yielded none within DMN nodes.

## Intranodal DMN Connectivity in Typically Developing Children versus Those With Autism Spectrum Disorder

The developmental disconnection model suggests that persons with ASD have a surfeit of local cortical connectivity, implying greater connectivity within DMN nodes and other functional networks in children with ASD. To make voxel-wise comparisons between ICA components in the $TD_{match}$ and ASD groups, we performed a dual-regression analysis on the resting-state data of each subject [Filippini et al., 2009]. We performed two-sample *t*-tests ($P < 0.05$; FWE corrected) on dual-regression derived maps based on the group-ICA components of the default mode, motor, and visual resting-state networks in both groups, using the $TD_{match}$ maps as a mask. Figure 3a shows the results of a comparison between DMN maps of both groups (ASD > $TD_{match}$). Comparisons between the ventral ACC/mPFC ASD component and the $TD_{match}$ component yielded a significant cluster located within the ACC/mPFC ROI. Similar results were obtained for not only the dorsal ACC/mPFC and PCC components but also for the motor (Fig. 3b) and visual networks (Fig. 3c). In both cases, these comparisons yielded a cluster of voxels located within the corresponding $TD_{match}$ ROI. Inverse comparisons ($TD_{match}$ > ASD) in the visual and motor networks as well as DMN revealed no significant voxels. These results demonstrate that children with ASD show higher functional connectivity within nodes of multiple resting-state networks, including DMN nodes, relative to TD children.

## Youngest (6–9 years) and Oldest (10–17 years) Typical Developing Children versus Children With Autism Spectrum Disorder

Having established functional connectivity differences between DMN nodes in the $TD_{match}$ and ASD groups, we compared the 12 youngest members of the $TD_{match}$ group, aged 6–9 years ($TD_{6–9}$ group, hereafter) to the whole ASD group. Figure 4a shows the results of ICA on the $TD_{6–9}$ group. BOLD activity associated with DMN spread across two separate component maps (2/19) in the $TD_{6–9}$ group. The predominant feature of one map was the ACC/mPFC and MTG nodes, and, in the other, the PCC and bilateral IPL nodes were predominant. For a more detailed comparison, we used ROI analyses to compare the $TD_{6–9}$ and ASD groups. Like above, all ROIs were based on nodes from the $TD_{match}$ group's single ICA component map because $TD_{match}$ ROIs account for each DMN node. Using a random effects ANOVA comparing the $TD_{6–9}$ group ($n = 12$) and the ASD group ($n = 24$), we found a main effect of ROI, such that connectivity between certain pairs of ROIs was greater than the connectivity between others ($F[14, 510] = 4.81$, $P < 0.01$). However, there was neither a main effect of group ($F[1, 510] = 0.27$, $P = 0.60$) nor an interaction of group and ROI pairings ($F[14, 510] = 0.86$, $P = 0.61$). These results show that although there are differences in the strength of functional connections between DMN nodes in the ASD and $TD_{6–9}$ groups, there are no group differences internodal DMN connectivity. The correlation matrix in Figure 4b is only shown for consistency because post-hoc analyses of insignificant ANOVA results are invalid.

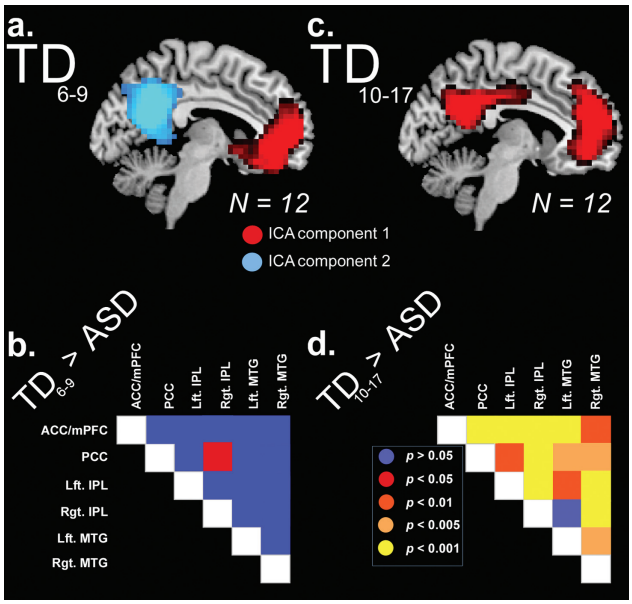


**Figure 4.**

(**a**) ICA component map of DMN functional connectivity in the $TD_{6–9}$ group superimposed onto the sagittal plane of a typical brain. Similar to the ASD group, more than one component is needed to capture the DMN network in the younger TD group. In this case, two ICA component maps were required to represent functional connectivity between DMN nodes in this group. (**b**) Correlation matrix of post-hoc comparisons of internodal DMN functional connectivity in the $TD_{6–9}$ and ASD groups. Colors are proportional to *P* values. The only statistically significant ($P < 0.05$) difference in connectivity between the $TD_{6–9}$ and ASD groups was the PCC and right IPL node pair. All differences correspond to the comparison of $TD_{6–9} >$ ASD. None of the connections were found to be significantly greater in the ASD group. (**c**) ICA component map of DMN functional connectivity in the $TD_{10–17}$ group superimposed onto the sagittal plane of a typical brain. Similar to the $TD_{match}$ group, the entire DMN network is captured by a single ICA component. (**d**) Correlation matrix of post-hoc comparisons of internodal DMN functional connectivity in the $TD_{10–17}$ and ASD groups. Unlike the $TD_{6–9}$ group, $TD_{10–17}$ group shows differences in connectivity throughout DMN. None of the connections were found to be significantly greater in the ASD group. Connectivity differences between the $TD_{6–9}$ and $TD_{10–17}$ groups and the ASD group are explained in more detail in Supporting Information Figures SS3 and SS4.

We also compared the functional connectivity between DMN nodes in the ASD group to that of the 12 oldest (aged 10–17 years) members of the $TD_{match}$ group ($TD_{10–17}$ group, hereafter). Figure 4c shows functional connectivity in a single ICA map (1/10) from the $TD_{10–17}$ group, and this single map accounts for each DMN node. A random effects ANOVA comparing the $TD_{10–17}$ group ($n = 12$) and the ASD group ($n = 24$) revealed main effects for both group ($F[1, 510] = 153.21$, $P < 0.01$) and ROI connectivity ($F[14, 510] = 1.87$, $P < 0.03$) but again no interaction thereof ($F[14, 510] = 0.90$, $P = 0.55$). As expected, these results imply that there are differences in the strength of functional connections between DMN nodes in the ASD group and the $TD_{10–17}$ group. Post-hoc tests showing functional connectivity differences between the ASD group and the $TD_{10–17}$ group are shown in Figure 4d. With the exception of left MTG and right IPL, significant differences between the ASD group and the $TD_{10–17}$ group were ubiquitous across internodal DMN connections. These analyses confirm that, in general the ASD group and $TD_{6–9}$ group have similarly weak functional connectivity relative to the $TD_{10–17}$ group.

## Modeling Functional Connectivity as a Function of Age

We ascertained differences in the development of DMN functional connectivity in children with ASD and age-matched typical developing children by modeling connectivity measures (Fisher's *Z*-scores from ROI analyses) from both the $TD_{match}$ and ASD groups against age. We fit second-order (quadratic) functions to each of our 16 node pairings (15 traditional DMN node pairs plus the dACC/mPFC and vACC/mPFC node pair). Of these, 13 $TD_{match}$ node pairings had model fits that significantly ($P < 0.05$) differed from zero (Fig. 5a). In the $TD_{match}$ group, only the functional connections between the PCC and right IPL, between right IPL and left MTG, and between left and right IPL did not increase as a quadratic function of age. The 13 significant model fits showed a marked, nonlinear increase in functional connectivity with increasing age, which either persists throughout the total age range studied (e.g., left IPL and left MTG), or plateaus (e.g., ACC/mPFC and left IPL), and/or slightly decreases (e.g., ACC/mPFC and PCC or dorsal ACC/mPFC and ventral ACC/mPFC). In children with ASD, model fits between age and connectivity were not significant (Fig. 5b), thus the functional connectivity between DMN nodes did not change as a function of age.

## Correlations Between Default Mode Connectivity and Autism Psychometrics

We investigated whether decreases in internodal DMN functional connectivity correlated with increased ASD symptoms using post-hoc analyses correlating internodal DMN functional connectivity in the ASD subjects with several autism psychometrics. A scatter-diagram of the internodal DMN functional connectivity of the PCC and right MTG for 17 subjects plotted against each subject's ADI-Soc score shows a significant relationship (Fig. 6a). A scatter diagram of internodal DMN functional connectivity of the ACC/mPFC and PCC for 10 subjects plotted against each subject's corresponding SRS–Mann subscore also

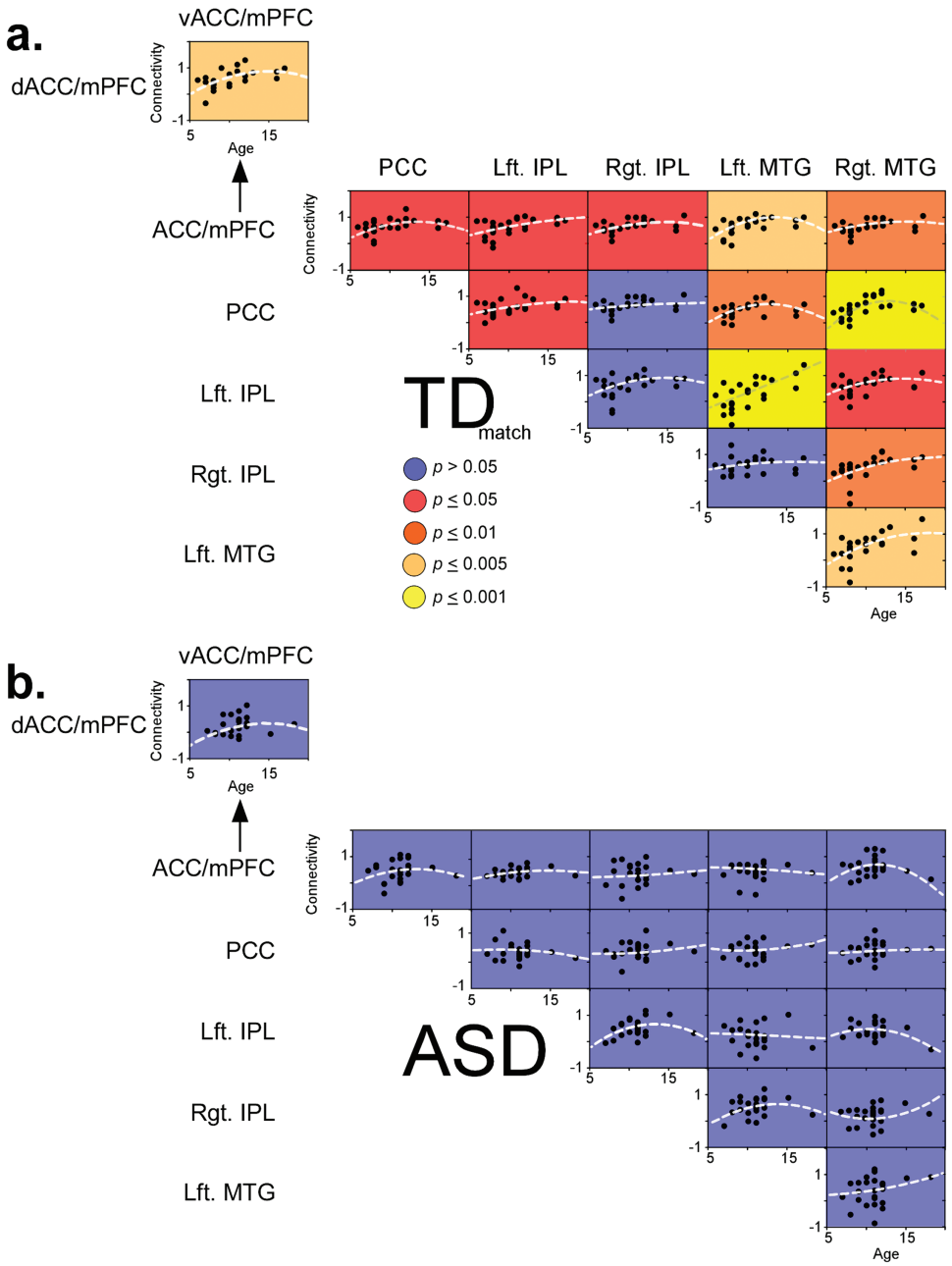


**Figure 5.**

Relationship between DMN functional connectivity and age. (**a**) Each of the 16 plots compares functional connectivity (Fisher's *Z*, ordinate) with the ages of children ($N = 24$, abscissa) in the $TD_{match}$ group. The upper left graph is a comparison between the dorsal and ventral portions of the ACC/mPFC region based on the ASD ICA. The remaining 15 graphs are comparisons between ROIs based on the same DMN nodes (ACC/mPFC, PCC, left IPL, right IPL, left MTG, and right MTG) as in Figures 3–5. Each black circle represents one child's functional connectivity. Each hashed, translucent line is the second-order fit. The background color of each plot indicates the significance of each second-order fit: blue indicates no correlation ($P > 0.05$), whereas red ($0.01 \leq P \leq 0.05$), red-orange ($0.005 \leq P \leq 0.01$), and yellow orange ($0.005 \leq P \leq 0.001$) indicate significant correlations, and yellow indicates the highest correlations ($P \leq 0.001$). (**b**) The same representation as "A" for the 24 children with ASD.

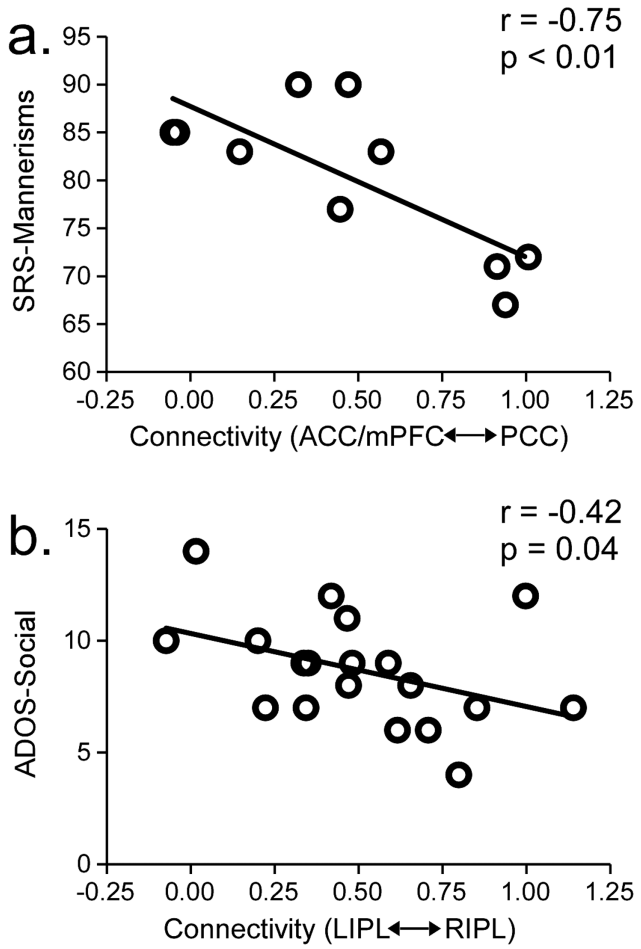


**Figure 6.**

Exploratory correlations between functional connectivity and ASD psychometrics. (**a**) Scatter diagram comparing the internodal DMN functional connectivity between the PCC and right MTG nodes (abscissa) in 17 children with ASD and the corresponding ADI Social (ADI-Soc) score (ordinate) for each subject. Correlations between PCC and right MTG connectivity and ADI-Soc scores showed an increase in symptom severity coinciding with decreased functional connectivity ($r = -0.50$). (**b**) Scatter-diagram comparing the internodal DMN functional connectivity between the ACC/mPFC and PCC nodes, expressed as Fisher's *Z*-scores (abscissa), in 10 children with ASD and the corresponding SRS Autistic Mannerism (SRS–Mann) score (ordinate) for each subject. Correlations between ACC/mPFC and PCC connectivity and SRS–Mann scores showed an increase in symptom severity coinciding with decreased functional connectivity ($r = -0.70$). Other significant correlations between internodal DMN connectivity and autism psychometrics are detailed in Supporting Information Table SS1.

revealed a significant correlation (Fig. 6b). These two scatter diagrams, as well as the other significant ($P < 0.05$) correlations summarized in Supporting Information Table SS1, illustrate how strongly differences in functional connectivity relate to symptoms of ASD. Note that these correlations above were (a) restricted to children with ASD as it is rare to administer them to TD children due to the time intensive nature of these tests and (b) one tailed as we only considered functional connections negatively correlated with autism psychometrics.

## DISCUSSION

The results presented here demonstrate that children with ASD fail to reach a stage of increasing long-distance cortical functional connectivity in the DMN at a time when TD children are developing most of their cortical synapses [Giedd et al., 1999; Gogtay et al., 2004]. There was also a surfeit of local connectivity within DMN nodes of these same children diagnosed with ASD. This double dissociation within DMN, a network associated with Theory of Mind [Saxe and Kanwisher, 2003; Spreng and Grady, 2010], episodic memory [Addis et al., 2007; Greicius and Menon, 2004; Kim et al., 2010], and prospection [Addis et al., 2007], provides support for the developmental disconnection model [Belmonte et al., 2004] and suggests that it may arise from a developmental delay.

While all but one [Monk et al., 2009] of the prior studies investigating internodal DMN functional connectivity in persons with ASD report decreased long distance connectivity [Assaf et al., 2010; Cherkassky et al., 2006; Kennedy and Courchesne, 2008; Wiggins et al., 2011], none included children younger than 10 years old and only one examined changes in functional connectivity as a function of age [Wiggins et al., 2011]. Results of these studies are largely consistent regarding reduced functional connectivity within DMN in ASD [Monk et al., 2009]. While one previous study examined developmental changes in connectivity and their findings are largely consistent with ours, their analyses focused only on identifying interactions between group and age [Wiggins et al., 2011]. By definition, such interaction effects preclude identifying any differences in connectivity where one group lacks a change in connectivity with age. Strikingly, our results match one finding showing equivalent brain volume in ASD and TD children at around 6–7 years of age, but, as they develop further, brain volume either plateaus or decreases in children with ASD but continues to increase in TD children [Courchesne et al., 2011]. In addition, our findings are consistent with studies showing reduced white matter volume in the corpus callosum in older persons with ASD relative to older TD persons, but not in younger (2–4 years old) TD persons and those with ASD [Ben Bashat et al., 2007; Boger-Megiddo et al., 2006]. These developmental changes may explain some of the inconsistencies between ASD connectivity studies [Wass, 2011].

A discussion of other potential influences on our data and data in similar studies is warranted. First, BOLD signals may be affected by baseline physiological conditions such as cerebral blood flow and respiration [Buxton, 2010;

Joel et al., 2011; Kim and Ogawa, 2012]. Such conditions may present problems when comparing typical children with those with ASD (and even other patient populations) because these populations may have drastically different physiological parameters at baseline. While it possible these physiological differences could exist and have an effect on our results, it would be unlikely given the fact that the differences in DMN connectivity only emerge in the older children. Another potential confound in our data is the fact that most of the autistic children in our study were on various psychoactive medications. It is common practice in autism research to perform neuroimaging studies on medicated children [Rudie et al., 2011; Scott-Van Zeeland et al., 2010]. Nevertheless, psychoactive medications may enhance, reduce, or not alter DMN functional connectivity. More relevant to our population, SSRIs and antipsychotics may reduce DMN connectivity [Abbott et al., 2011; Delaveau et al., 2010], but psychostimulants normalize the relationship between the DMN and the executive function network [Peterson et al., 2009]. Given the various and often conflicting effects of these drugs on DMN, it would appear unlikely that their cumulative effect would be to decrease internodal DMN connectivity and increase intranodal connectivity in the visual and motor networks as well as DMN. Reduced long-distance connectivity that is only exhibited in the older ASD children combined with increased local connectivity is unlikely to be the result of a pharmacological effect. Finally, caution is needed with regards to the interpretation of the post-hoc correlations with the autism psychometric measures given the small sample sizes. These correlations nonetheless suggest that the differences in connectivity demonstrated within the DMN could be related to the specific factors of the disorder, namely those related to social-communication deficits.

Proponents of the developmental disconnection model [Belmonte et al., 2004; Just et al., 2004] use it to explain deficits in various forms of neural processing among persons with ASD. Some deficits associated with a surfeit of local connectivity include motor coordination deficits [Teitelbaum et al., 1998] and exceedingly high thresholds of visual motion coherence [Milne et al., 2002]. Insofar as long-distance connectivity is concerned, coordinating neural activity between the six distinct nodes of the DMN requires long distance connections of either a direct synaptic or correlatively computational nature [Belmonte et al., 2004]. A recent postmortem study demonstrated that, relative to typically developed adults, those with ASD have decreased long-distance and increased short-distance axonal connections within frontal cortex regions related to DMN, including the ACC [Zikopoulos and Barbas, 2010]. A dissociation between gray and white matter growth in boys further supports this model [Hua et al., 2011]. A recent study demonstrating reduced functional connectivity of the medial prefrontal cortex in at risk carriers of the CNTNAP2 gene provides a possible genetic underpinning to these findings [Scott-Van Zeeland et al., 2010]. Our results indicate that the connectivity deficits in ASD within the DMN occur as a result of a lack of developmental strengthening of connectivity within this network. Notably, in the 6–9 year olds, there are no group differences in connectivity within this network. Rather, these differences occur later in development. The results we report support the developmental disconnection model and suggest an interesting, possible explanation of the Theory-of-Mind hypothesis of autism.

## ACKNOWLEDGMENTS

The authors are indebted to the children who participated in this study and to their families. The authors are grateful for the contributions of Lauren Kenworthy, PhD, who, in her role as Director of the Center for Autism Spectrum Disorder at Children's National Medical Center, oversaw the assessment of the autism-related behavioral data (e.g., ADOS, ADI-R, etc.) presented here. Rusan Chen, PhD, generously gave helpful advice on statistical analyses. The authors acknowledge Thomas Zeffiro, MD, PhD, as the initial principal investigator of the Georgetown program project of the Kennedy Krieger Institute Studies to Advance Autism Research and Treatment (STAART) Grant. The authors thank Vittorio Gallo, PhD, for providing helpful feedback on this manuscript and Paul R. A. Robinson for technical assistance with the GNU Blender 2.65 3D rendering program..

## REFERENCES

Abbott C, Juarez M, White T, Gollub RL, Pearlson GD, Bustillo J, Lauriello J, Ho B, Bockholt HJ, Clark VP, Magnotta V, Calhoun VD (2011): Antipsychotic dose and diminished neural modulation: A multi-site fMRI study. Prog Neuropsychopharmacol Biol Psychiatry 35:473–482.

Addis DR, Wong AT, Schacter DL (2007): Remembering the past and imagining the future: Common and distinct neural substrates during event construction and elaboration. Neuropsychologia 45:1363–1377.

Assaf M, Jagannathan K, Calhoun VD, Miller L, Stevens MC, Sahl R, O'Boyle JG, Schultz RT, Pearlson GD (2010): Abnormal functional connectivity of default mode sub-networks in autism spectrum disorder patients. Neuroimage 53:247–256.

Baron-Cohen S (1989): The theory of mind hypothesis of autism: A reply to Boucher. Br J Disord Commun 24:199–200.

Beckmann CF, DeLuca M, Devlin JT, Smith SM (2005): Investigations into resting-state connectivity using independent component analysis. Philos Trans R Soc Lond B Biol Sci 360:1001–1013.

Beckmann CF, Smith SM (2005): Tensorial extensions of independent component analysis for multisubject FMRI analysis. Neuroimage 25:294–311.

Belmonte MK, Allen G, Beckel-Mitchener A, Boulanger LM, Carper RA, Webb SJ (2004): Autism and abnormal development of brain connectivity. J Neurosci 24:9228–9231.

Belmonte MK, Yurgelun-Todd DA (2003): Functional anatomy of impaired selective attention and compensatory processing in autism. Brain Res Cogn Brain Res 17:651–664.

Ben Bashat D, Kronfeld-Duenias V, Zachor DA, Ekstein PM, Hendler T, Tarrasch R, Even A, Levy Y, Ben Sira L (2007): Accelerated maturation of white matter in young children with autism: A high b value DWI study. Neuroimage 37:40–47.

Ben Shalom D (2003): Memory in autism: Review and synthesis. Cortex 39:1129–1138.

Boger-Megiddo I, Shaw DW, Friedman, SD, Sparks BF, Artru AA, Giedd JN, Dawson G, Dager SR (2006): Corpus callosum morphometrics in young children with autism spectrum disorder. J Autism Dev Disord 36:733–739.

Boucher J (1989): The theory of mind hypothesis of autism: Explanation, evidence and assessment. Br J Disord Commun 24:181–198.

Brett M, Anton J-L, Valabregue R, Poline J.Region of interest analysis using an SPM toolbox [abstract]. Presented at the 8th International Conference on Functional Mapping of the Human Brain, June 2–6, 2002, Sendai, Japan.

Buckner RL, Andrews-Hanna JR, Schacter DL (2008): The brain's default network: Anatomy, function, and relevance to disease. Ann N Y Acad Sci 1124:1–38.

Buxton RB (2010): Interpreting oxygenation-based neuroimaging signals: The importance and the challenge of understanding brain oxygen metabolism. Front Neuroenergetics 2:8.

Cherkassky VL, Kana RK, Keller TA, Just MA (2006): Functional connectivity in a baseline resting-state network in autism. Neuroreport 17:1687–1690.

Colle L, Baron-Cohen S, Hill J (2007): Do children with autism have a theory of mind? A non-verbal test of autism vs. specific language impairment. J Autism Dev Disord 37:716–723.

Comon P (1994): Independent component analysis, A new concept?Signal Process 36:287–314.

Constantino JN, Gruber CP (2005): Social Responsiveness Scale (SRS). Western Psychological Services, Los Angeles, CA

Courchesne E, Campbell K, Solso S (2011): Brain growth across the life span in autism: Age-specific changes in anatomical pathology. Brain Res 1380:138–145.

Dahlgren S, Dahlgren Sandberg A, Larsson M (2010): Theory of mind in children with severe speech and physical impairments. Res Dev Disabil 31:617–624.

Damarla SR, Keller TA, Kana RK, Cherkassky VL, Williams DL, Minshew NJ, Just MA (2010): Cortical underconnectivity coupled with preserved visuospatial cognition in autism: Evidence from an fMRI study of an embedded figures task. Autism Res 3:273–279.

Delaveau P, Jabourian M, Lemogne C, Guionnet S, Bergouignan L, Fossati P (2010): Brain effects of antidepressants in major depression: A meta-analysis of emotional processing studies. J Affect Disord 130:66–74.

Fair DA, Schlaggar BL, Cohen AL, Miezin FM, Dosenbach NU, Wenger KK, Fox MD, Snyder AZ, Raichle ME, Petersen SE (2007): A method for using blocked and event-related fMRI data to study "resting state" functional connectivity. Neuroimage 35:396–405.

Fair DA, Cohen AL, Dosenbach NU, Church JA, Miezin FM, Barch DM, Raichle ME, Petersen SE, Schlaggar BL (2008): The maturing architecture of the brain's default network. Proc Natl Acad Sci U S A 105:4028–4032.

Filippini N, MacIntosh BJ, Hough MG, Goodwin GM, Frisoni GB, Smith SM, Matthews PM, Beckmann CF, Mackay CE (2009): Distinct patterns of brain activity in young carriers of the APOE-epsilon4 allele. Proc Natl Acad Sci USA 106:7209–7214.

Geschwind DH, Levitt P (2007): Autism spectrum disorders: Developmental disconnection syndromes. Curr Opin Neurobiol 17:103–111.

Giedd JN, Blumenthal J, Jeffries NO, Castellanos FX, Liu H, Zijdenbos A, Paus T, Evans AC, Rapoport JL (1999): Brain development during childhood and adolescence: A longitudinal MRI study. Nat Neurosci 2:861–863.

Gogtay N, Giedd JN, Lusk L, Hayashi KM, Greenstein D, Vaituzis AC, Nugent TF, 3rd, Herman DH, Clasen LS, Toga AW, Rapoport JL, Thompson PM (2004): Dynamic mapping of human cortical development during childhood through early adulthood. Proc Natl Acad Sci USA 101:8174–8179.

Gordon EM, Lee PS, Maisog JM, Foss-Feig J, Billington ME, VanMeter J, Vaidya CJ (2011): Strength of default mode resting-state connectivity relates to white matter integrity in children. Dev Sci 14:738–751.

Greicius MD, Krasnow B, Reiss AL, Menon V (2003): Functional connectivity in the resting brain: A network analysis of the default mode hypothesis. Proc Natl Acad Sci USA 100:253–258.

Greicius MD, Menon V (2004): Default-mode activity during a passive sensory task: Uncoupled from deactivation but impacting activation. J Cogn Neurosci 16:1484–1492.

Hua X, Thompson PM, Leow AD, Madsen SK, Caplan R, Alger JR, O'Neill J, Joshi K, Smalley SL, Toga AW, Levitt JG (2011): Brain growth rate abnormalities visualized in adolescents with autism. Hum Brain Mapp. (Epub ahead of print).

Joel SE, Caffo BS, van Zijl PC, Pekar JJ (2011): On the relationship between seed-based and ICA-based measures of functional connectivity. Magn Reson Med 66:644–657.

Just MA, Cherkassky VL, Keller TA, Minshew NJ (2004): Cortical activation and synchronization during sentence comprehension in high-functioning autism: Evidence of underconnectivity. Brain 127:1811–1821.

Kennedy DP, Courchesne E (2008): The intrinsic functional organization of the brain is altered in autism. Neuroimage 39:1877–1885.

Kim H (2010): Dissociating the roles of the default-mode, dorsal, and ventral networks in episodic memory retrieval. Neuroimage 50:1648–1657.

Kim H, Daselaar SM, Cabeza R (2010): Overlapping brain activity between episodic memory encoding and retrieval: Roles of the task-positive and task-negative networks. Neuroimage 49:1045–1054.

Kim SG, Ogawa S (2012): Biophysical and physiological origins of blood oxygenation level-dependent fMRI signals. J Cereb Blood Flow Metab 32:1188–1206.

Kiviniemi V, Starck T, Remes J, Long X, Nikkinen J, Haapea M, Veijola J, Moilanen I, Isohanni M, Zang YF, Tervonen O (2009): Functional segmentation of the brain cortex using high model order group PICA. Hum Brain Mapp 30:3865–3886.

Lackner CL, Bowman LC, Sabbagh MA (2010): Dopaminergic functioning and preschoolers' theory of mind. Neuropsychologia 48:1767–1774.

Lenroot RK, Giedd JN (2006): Brain development in children and adolescents: Insights from anatomical magnetic resonance imaging. Neurosci Biobehav Rev 30:718–729.

Lombardo MV, Chakrabarti B, Bullmore ET, Wheelwright SJ, Sadek SA, Suckling J, Baron-Cohen S (2010): Shared neural circuits for mentalizing about the self and others. J Cogn Neurosci 22:1623–1635.

Lord C, Risi S, Lambrecht L, Cook EH, Jr., Leventhal BL, DiLavore PC, Pickles A, Rutter M (2000): The autism diagnostic

observation schedule-generic: A standard measure of social and communication deficits associated with the spectrum of autism. J Autism Dev Disord 30:205–223.

Lord C, Rutter M, Le Couteur A (1994): Autism Diagnostic Interview-Revised: A revised version of a diagnostic interview for caregivers of individuals with possible pervasive developmental disorders. J Autism Dev Disord 24:659–685.

Milne E, Swettenham J, Hansen P, Campbell R, Jeffries H, Plaisted K (2002): High motion coherence thresholds in children with autism. J Child Psychol Psychiatry 43:255–263.

Monk CS, Peltier SJ, Wiggins JL, Weng SJ, Carrasco M, Risi S, Lord C (2009): Abnormalities of intrinsic functional connectivity in autism spectrum disorders. Neuroimage 47:764–772.

Penagarikano O, Abrahams BS, Herman EI, Winden KD, Gdalyahu A, Dong H, Sonnenblick LI, Gruver R, Almajano J, Bragin A, Golshani P, Trachtenberg JT, Peles E, Geschwind DH (2011): Absence of CNTNAP2 Leads to epilepsy, neuronal migration abnormalities, and core autism-related deficits. Cell 147:235–246.

Peterson BS, Potenza MN, Wang Z, Zhu H, Martin A, Marsh R, Plessen KJ, Yu S (2009): An FMRI study of the effects of psychostimulants on default-mode processing during Stroop task performance in youths with ADHD. Am J Psychiatry 166:1286–1294.

Raichle ME, MacLeod AM, Snyder AZ, Powers WJ, Gusnard DA, Shulman GL (2001): A default mode of brain function. Proc Natl Acad Sci U S A 98:676–682.

Rudie JD, Shehzad Z, Hernandez LM, Colich NL, Bookheimer SY, Iacoboni M, Dapretto M (2011): Reduced functional integration and segregation of distributed neural systems underlying social and emotional information processing in autism spectrum disorders. Cereb Cortex 22:1025–1037.

Saxe R, Kanwisher N (2003): People thinking about thinking people. The role of the temporo-parietal junction in "theory of mind". Neuroimage 19:1835–1842.

Scott-Van Zeeland AA, Abrahams BS, Alvarez-Retuerto AI, Sonnenblick LI, Rudie JD, Ghahremani D, Mumford JA, Poldrack RA, Dapretto M, Geschwind DH, Bookheimer SY (2010): Altered functional connectivity in frontal lobe circuits is associated with variation in the autism risk gene CNTNAP2. Sci Transl Med 2:56ra80.

Spreng RN, Grady CL (2010): Patterns of brain activity supporting autobiographical memory, prospection, and theory of mind, and their relationship to the default mode network. J Cogn Neurosci 22:1112–1123.

Stigler KA, McDonald BC, Anand A, Saykin AJ, McDougle CJ (2011): Structural and functional magnetic resonance imaging of autism spectrum disorders. Brain Res.

Teitelbaum P, Teitelbaum O, Nye J, Fryman J, Maurer RG (1998): Movement analysis in infancy may be useful for early diagnosis of autism. Proc Natl Acad Sci U S A 95:13982–13987.

Tyler CW, Kontsevich LL, Ferree TC (2008): Independent components in stimulus-related BOLD signals and estimation of the underlying neural responses. Brain Res 1229:72–89.

Van Dijk KR, Hedden T, Venkataraman A, Evans KC, Lazar SW, Buckner RL (2010): Intrinsic functional connectivity as a tool for human connectomics: Theory, properties, and optimization. J Neurophysiol 103:297–321.

Wass S (2011): Distortions and disconnections: Disrupted brain connectivity in autism. Brain Cogn 75:18–28.

Wiggins JL, Peltier SJ, Ashinoff S, Weng SJ, Carrasco M, Welsh RC, Lord C, Monk CS (2011): Using a self-organizing map algorithm to detect age-related changes in functional connectivity during rest in autism spectrum disorders. Brain Res 1380:187–197.

Zikopoulos B, Barbas H (2010): Changes in prefrontal axons may disrupt the network in autism. J Neurosci 30:14595–14609.